RSC Advances

REVIEW

View Article Online
View Journal | View Issue



Cite this: *RSC Adv.*, 2020, **10**, 12851

# Development of hydrophobic reduced graphene oxide as a new efficient approach for photochemotherapy†

Seyyed Mojtaba Mousavi,[a] Foo Wah Low,*[b] Seyyed Alireza Hashemi,[c] Nurul Asma Samsudin,[b] Mohammad Shakeri,[b] Yulisa Yusoff,[b] Mansoor Rahsepar,[d] Chin Wei Lai,*[e] Aziz Babapoor,[f] Sadaf Soroshnia,[f] Su Mei Goh,[f] Sieh Kiong Tiong[g] and Nowshad Amin[b]

Received 8th January 2020
Accepted 9th March 2020

DOI: 10.1039/d0ra00186d

rsc.li/rsc-advances

Nowadays, chemotherapy is one of the crucial and common therapies in the world. So far, it has been revealed to be highly promising, yet patients suffer from the consequences of severe negative medical dosages. In order to overcome these issues, the enhancement of photothermal chemotherapy with reduced graphene oxide (rGO) as a photothermal agent (PTA) is widely utilised in current medical technologies. This is due to its high near-infrared region (NIR) response, *in vitro* or *in vivo* organism biocompatibility, low risk of side effects, and effective positive results. Moreover, rGO not only has the ability to ensure that selective cancer cells have a higher mortality rate but can also improve the growth rate of recovering tissues that are untouched by necrosis and apoptosis. These two pathways are specific diverse modalities of cell death that are distinguished by cell membrane disruption and deoxyribonucleic acid (DNA) disintegration of the membrane *via* phosphatidylserine exposure in the absence of cell membrane damage. Therefore, this review aimed to demonstrate the recent achievements in the modification of rGO nanoparticles as a PTA as well as present a new approach for performing photochemotherapy in the clinical setting.



## 1. Introduction

According to the World Health Organisation (WHO) data regarding the burden of cancer, an estimated 9.6 million deaths (ratio of 1 : 8 for men and 1 : 11 for women) were recorded in 2018 worldwide. Photothermal therapy (PTT) is a form of nanotechnology and it is noted as the most significant therapeutic method in utilising heat and having strong absorption in the near-infrared (NIR) region for cancer ablation purposes.[1] Researchers have demonstrated the efficacy of many PTT agents in destroying cancer cells, such as the use of carbon nanomaterials as a theragnostic agent. However, laser irradiation in high doses can dramatically destroy the adjoining tissues. Besides, carbon nanomaterials coated with noble metal nanoparticles (gold and silver) are not biodegradable and may cause toxicity during treatment.

The development of nanoparticles with an abundance of purposes has been the subject of research and clinical field in recent decades. For cancer imaging and diagnosis, the usage of nanoparticles in either intrinsic biological factors of cancer or therapeutic functionalities are highly appreciated.[2–10] By adopting nanoparticle materials in therapies, some toxic chemicals (*e.g.*, dyes and drugs) can be easily eliminated in cancer diagnostics and treatments. Besides, fluorescent molecular dyes are potentially an incorrect option for medical purposes as they can cause various negative effects due to their inherent toxicity. Recently, nanoparticles with functionalised carbon family networks have shown great promise for cancer targeting and drug delivery in specific chemotherapy treatments, such as carbon dots, carbon nanotubes (CNTs), fullerenes, and graphene materials.[11–16] Among these carbon nanomaterials, graphene is the most suitable and commonly used material in a variety of applications due to its sheet

[a]*Department of Chemical Engineering, National Taiwan University of Science and Technology, Taiwan*
[b]*Institute of Sustainable Energy, Universiti Tenaga Nasional (@The Energy University), Jalan IKRAM-UNITEN, 43000 Kajang, Selangor, Malaysia. E-mail: lowfw@uniten.edu.my*
[c]*Department of Mechanical Engineering, Center for Nanofibers and Nanotechnology, National University of Singapore, Singapore*
[d]*Department of Materials Science and Engineering, School of Engineering, Shiraz University, Shiraz, Iran*
[e]*Nanotechnology & Catalysis Research Centre, Level 3, Block A, Institute for Advanced Studies Building, University of Malaya, 50603 Kuala Lumpur, Malaysia. E-mail: cwlai@um.edu.my*
[f]*Department of Chemical Engineering, University of Mohaghegh Ardabili (UMA), Ardabil, Iran*
[g]*College of Engineering, Universiti Tenaga Nasional (@The Energy University), Jalan IKRAM-UNITEN, 43000 Kajang, Selangor, Malaysia*

† Electronic supplementary information (ESI) available. See DOI: 10.1039/d0ra00186d

flexibility. It is capable of generating heat by alternating the magnetic field or through lasers of noble metals.[17,18]

Nowadays, different specific structures of graphene oxide (GO) have been numerously prepared *via* different ways and with different extents of oxidation. In general, strong photoluminescence can be produced from GO with either wave laser access, a pulsed laser (visible range), or NIR wavelength conditions; the outcome will be dye-free labelling cells for diagnostics. In fact, the concensus is that GO consists of many functionalised groups, whereby a majority of them comprise carboxylic and hydroxylic groups. This demonstrates their surface functionalisation role for numerous applications, such as drug delivery and biosensing.[19,20] Specifically, graphene is defined as a two-dimensional (2D) basal planar structure with a one-atom thickness of approximately 0.35–1.6 nm per layer. It shows a trigonal hybridisation of the carbon–carbon atom bonds, which are firmly arranged into a honeycomb crystal network.[21] Moreover, graphene exhibits doubled larger surface area than CNTs, rendering it applicable as a drug carrier agent. In addition, the graphene material is highly recommended as a drug carrier agent due to its hydrophobic behaviour. Su *et al.* revealed that preparing it by a chemical reduction method can prevent its aggregation.[22]

Upon oxidation, the stacked graphene sheets of a carbonaceous structure will break up and generate flaws that are visible as clear stacked wrinkles, and which significantly increase the adjacent sheet distance from 3.35 Å to 6.8 Å for graphite and GO, respectively. The increased spacing is affected by its water intercalation and results in the delamination of GO into multiple individual GO sheets under low-power sonication in water. For pH measurement, negatively charged oxygenated functional groups on the GO surface will remain even though they are produced in an aqueous solution. Besides, it promises other outstanding properties, such as low production cost, a large surface area for drug absorption and low toxic metallic contaminations from the preparation process.[23] In addition, GO and its composites have been shown to achieve a considerably improved tumour targeting effect and higher tumour uptake due to enhanced permeability and their retention effects compared to CNTs, which are assumed to be due to their special features of a 2D structure and thin lateral size.[24–27] Apart from this, reduced graphene oxide (rGO) embraces a unique structure, which shows strong interaction between the carbon–carbon interlayers and exhibits low energy photons in the infrared region (*i.e.* approaching X-rays and gamma rays).

Remarkably, graphene has shown the capability to give a good response under specific wavelengths, such as NIR, and demonstrates plasmonic effects, which means it can generate heat *via* the plasmonic photothermal energy conversion route. When irradiated under NIR, graphene surface plasmons will induce a random dipole, while its resonance will be transmitted, which can be used to tune the thermal photon energy to gain a better output. Therefore, graphene-based materials are known as excellent photothermal agents (PTAs) for PTT. For rGO, its photothermal conversion efficiency is derived by the chemical reduction from GO, namely with the partially reinstated aromatic character of the graphene sheets. Interestingly, its NIR absorbance can be improved by up to six times compared to GO due to its highly intact aromatic structure.[28] Gonçalves and co-workers proved that an extremely small amount of nano-GO (*i.e.* 0.0005 mg $mL^{-1}$) could transfer energy from particles to a specific solution *via* radiation (*i.e.* under irradiation at 980 nm laser with an intensity of $1.0 \times 10^5$ W $m^{-2}$).[29] In fact, rGO itself is rich of oxygenated atoms as it approaches the site of defect, it still raises from the coupling of electronic states against the asymmetric stretch mode and thus considerably improves the infrared absorption for PTT.[30,31]

Commonly, cancer disease treatments *via* PTT facilities involving photosensitising agents utilise their own cells to produce heat from light absorption. Further harvesting for photoablation will result in both the living cancer cells and healthy cells being led to their death.[32,33] In order to prevent healthy cells from being heated, photosensitisers must be developed for high NIR absorption and for selective cancer-causing tumour cell death over healthy cells and tissues. The sharp penetration and minor nonspecific and non-uniform distribution of photothermal heating in the NIR window can result in lower light absorption by the tissues and in greater transparency within the optical window.[34] In particular, novel materials with high optical absorbance in the NIR region for PTT include gold nanoshells,[34] gold nanorods[35,36] and CNTs.[37–39] In Table 1, the photothermal therapies utilising different materials and an 808 nm diode laser are demonstrated with the effective laser intensity of 0.7–9.2 W $cm^{-2}$.

This paper reviews the recent developments of metabolic imaging systems for photochemotherapy using 2D carbon materials of graphene and graphene-based conjugates for cancer disease healing purposes. Briefly, the graphene strategies are summarised into three main sections: (i) rGO preparation methods, (ii) photothermal chemotherapy applications and (iii) future perspective of PTT using rGO. Furthermore, the future perspective of PTT *via* graphene strategies for drug carrier anticancer treatment is described accordingly. This work addresses the use of graphene nanomaterials in a biomedical perspective for bioimaging and theranostic tools over the last couple of years (Table 1). In this comprehensive work, the promising approaches, limitations and challenges in the field of cancer treatment are assessed *via* graphene-incorporated imaging tools/drugs delivery.

## 2. Reduced graphene oxide preparation methods

Generally, rGO is produced from GO or exfoliated graphite oxide *via* chemical or thermal reductive approaches. Some of the specific surface areas and capacitors that thermally and chemically reduce GO are summarised and listed in Table 2. From the short description, rGO is defined as an intermediate structure between ideal graphene and partially oxidised GO.[49] It is not only applicable to the biomedical field but also in other fields. Further physicochemical properties of the materials containing GO are listed in Fig. 1 and Table 3.

 

Table 1 Summary of some photothermal cancer therapy-based graphene materials

| Nanoconjugates | Modified materials | Particle sizes (nm) | Laser | Power density (W $cm^{-2}$) | Drug/imaging molecules used | Model | Performances | References |
|---|---|---|---|---|---|---|---|---|
| Polydopamine functionalised reduced graphene oxide (pRGO) with hyaluronic acid (HA) coated mesoporous silica (MS) pRGO@MS-HA | MS-HA | ~200 | 808 nm NIR laser | 1.5 | Doxorubicin (DOX) | *In vitro* and *in vivo* | Efficient synergistic targeted chemo-PTT, has minimal cytotoxicity. Good specificity to target tumour cells | 40 |
| Alanine incorporated functionalised graphene oxide (ARGO) | Alanine | — | 808 nm NIR laser | 2.5 | U87-MG | *In vitro* | Functional groups allow more accurate targeting in PTT without damaging tissue and healthy cells | 41 |
| Nano graphite oxide (nGO) | Gluthathione (GSH) | ~50 | 808 nm NIR laser | 3.0 | DOX | *In vitro* | Higher cancer cell death efficacy | 42 |
| Artesunate (ARS) modified PEGylated nanographene oxide (nGO-PEG), nGO-PEG-ARS | ARS | 182 | 808 nm NIR laser | 2.0 | Reactive oxygen species (ROS) and peroxynitrite (ONOO) | *In vitro* and *in vivo* | Faster tumour cure process | 43 |
| rGO | rGO | ~100 | 980 nm laser | 0.5–0.75 | Panc02-H7 | *In vivo* | Enable obtaining the desired thermal destruction effect on mice pancreatic cancers | 44 |
| rGO-hyaluronic acid (HA)-based amphiphilic polymer | Amphiphile | 108 ± 51 | 808 nm NIR light | 1.7 | CD44 | *In vitro* | Induced cancer cell's ablation | 45 |
| Polyethylene glycol functionalised rGO with gold (Au) nanorods Au NRs@rGO-PEG | Au nanorods | ~100 | 800 nm | 0.7 | Glioblastoma astrocytoma (U87MG) | *In vitro* and *in vivo* | Significant drop in tumour size after 5 days | 46 |
| Nanographene oxide methylene blue platform (NanoGO-MB) | MB | >100 | 808 nm NIR laser | 9.2 | NIH/3T3 and 4T1 | *In vitro* and *in vivo* | All tumours defeated once PDT/PTT were combined | 47 |
| Immobilised antiarrhythmic peptide 10 (APP10) decorated with dopamine-modified rGO (AAP10-pDA/rGO) | AAP10 | ~300 | 808 nm NIR laser | 1.5 | MCF-10A, MCF-7, and 4T1 | *In vitro* and *in vivo* | Improved the therapeutic efficiency against the bystander effect | 48 |

Previously, Becerril *et al.*[64] tried to reduce GO films at 1000 °C by using the thermal annealing method and discovered the ideal vacuum level was at $<10^5$ Torr for GO recovery. At that particular moment, the film will rapidly disappear *via* a reaction with the residual oxygen throughout the system. Moreover, inert atmospheres are one of the essential factors of concern; for example, reducing hydrogen gas ($H_2$) is typically provided to eliminate the residual oxygen. In addition, $H_2$ is especially used for its high reducing abilities for the reduction of GO, which can be achieved at a low temperature under a $H_2$ atmosphere.

Table 2 Chemical and thermal production of graphene

| Type of graphene | Reinforced materials | Methods | Size obtained (nm) | Conductivity (S $m^{-1}$) | Application | Ref. |
|---|---|---|---|---|---|---|
| rGO | Epoxy resin polymer | Chemical | 60 | — | Electromagnetic interference shielding and microwave-absorbing | 50 |
| rGO | L-Ascorbic acid | Chemical and mechanical | 24.49 | 7640 | — | 51 |
| rGO | Titanium dioxide | Chemical | 47 | 11.2 μ | Dye-sensitised solar cells | 52–55 |
| rGO | Glassy carbon | Chemical | — | — | Neurotransmitter | 56 |
| rGO | Titanium dioxide | Mechanical | 25 | — | Fibre-shaped dye-sensitised solar cells | 57 |
| rGO | — | Mechanical | 84.1 | — | Neural repair | 58 |

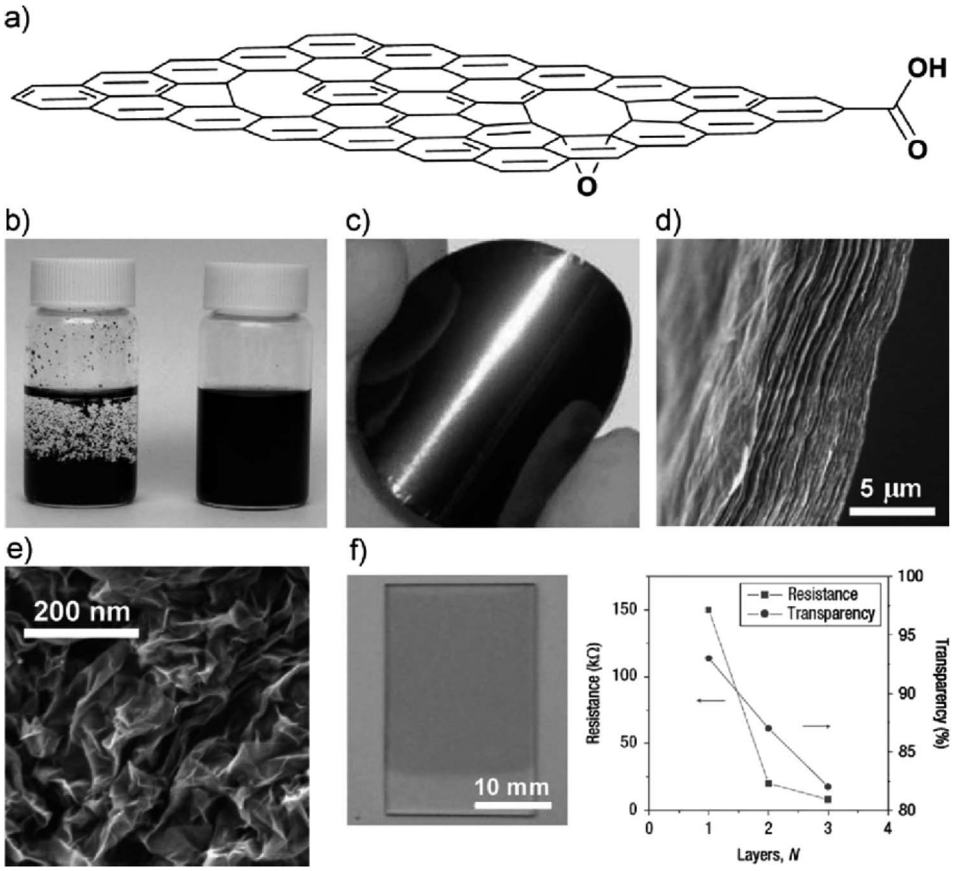


Fig. 1 (a) Schematic diagram of a highly oxidised rGO sheet, (b) photograph of aqueous solutions of graphene sheets reduced in the absence (left) and presence (right) of poly(sodium4-styrenesulfonate) (PSS),[59] (c) image of a graphene sheet,[60] (d) cross-sectional view of graphene paper layered structure,[61] (e) morphological view of aggregated graphene sheets in the form of graphene powder,[62] (f) transparent conductive graphene thin film fabricated *via* Langmuir–Blodgett assembly with plot results.[63]

Furthermore, Wu *et al.* reported that GO was easily reduced under an $Ar/H_2$ mixture (1 : 1) access for 2 h at 450 °C with a C/O ratio of 14.9, ultimately achieving a conductivity of up to ~1100 S $cm^{-1}$. Besides, Li *et al.*[65] demonstrated that GO could be synthesised in low-pressure ammonia mixture (*i.e.* 2 Torr $NH_3$/Ar (10% $NH_3$)) *via* the thermal annealing technique. In other preparatory methods, GO can also be reduced through photochemical reactions with the assistance of an active metal oxide photocatalyst (*i.e.* titanium dioxide ($TiO_2$)). Recently, Williams *et al.* demonstrated reducing GO *via* integrated $TiO_2$ particles under ultraviolet (UV) irradiation, whereby the indicator colour immediately changed from bright brown to dark brown and then to black.[66] This tuned colour suggests the partial restoration of the conjugated network in the respective carbon basal planes, similar to with the chemical reduction processes.

Table 3 Physicochemical properties of various types of graphene

| Properties | Monolayer graphene | GO | rGO |
|---|---|---|---|
| Young's modulus | 1 TPa | 207.6 GPa | — |
| Tensile strength | 130 GPa | 37.9 MPa | — |
| Optical transmittance | 97.7% | 24.8% | (60–90% depending on the reduction agent and synthesis method) |
| Charge carrier density | $8.7 \times 10^{12}$ $cm^{-2}$ | — | — |
| Charge mobility (ambient temperature) | 200 000 $cm^2$ $V^{-1}$ $s^{-1}$ | — | 372 $cm^2$ $V^{-1}$ $s^{-1}$ |
| Thermal conductivity | 2000–5000 W m $K^{-1}$ | 2000 W m $K^{-1}$ for uncontaminated 600 W m $K^{-1}$ on $Si/SiO_2$ substrate | 8.8 W m $K^{-1}$ |
| Electrical conductivity | 700 S $cm^{-1}$ | <1 μS $cm^{-1}$ | 200–35 000 S $cm^{-1}$ |

 

Meanwhile, An and co-workers[67] employed the electrophoretic deposition method (EPD) to produce GO films. During the EPD process, they aimed to reduce the GO sheets for the anode surface, which was counter-intuitive to the assumption that oxidation occurred at the anode as an electrolysis cell. Although the reduction reaction is yet to be fully discovered, assembling the films and simultaneously reducing them may be particularly attractive in some electrochemical applications. In another research, Dubin *et al.*[67] reported that the reduction of graphene while applying the *N*-methyl-2-pyrrolidinone (NMP) solvent as a modification may be done for the solvothermal approach. The method is totally different from the common synthesis route in which the reduction of graphene is performed in a non-sealed container. In addition, the samples were heated at the temperature of 200 °C, which was 2 °C lower than the actual boiling point of NMP (202 °C, 1 atm). In this comprehensive experiment, no further additional pressure was needed in the reduction process. The established deoxygenation of GO notes that the NMP solvent can be combined with its's moderate thermal annealing and oxygen-scavenging properties at high temperature. Nonetheless, the electrical conductivity performance and subsequent vacuum filtration of the rGO films was measured as 3.74 S $cm^{-1}$ for the solvothermal reduction method, which was exactly one order of magnitude smaller than for the hydrazine solvent reduction method (82.8 S $cm^{-1}$). The carbon to oxygen (C : O) ratio *via* solvothermal-reduced GO was just 5.15, which was also inferior to other results. Thus, the solvothermal reduction method is considered a moderate reduction method for GO. Regardless, it has shown much more suitable results by creating a stable dispersion of rGO sheets, which is worthwhile for usable applications.

## 3. Photothermal chemotherapy and the biomedical applications of rGO

rGO has been widely used for biomedical applications across a wide range over the past few years. For instance, photo-responsive indocyanine green-loaded GO nanosheets are known as a theranostic nanoplatform for photoacoustic imaging guiding and synergistic PTT treatments. They have the ability to enhance the PTT efficiency with cancer-targeting by increasing the photostability in the presence of folic acid (FA) conjugation for cancer therapies. Nevertheless, it has been revealed that fluorescent methods using organic dyes have several limitations, including dye degradation, photobleaching and a set limitation beyond clinical applications. To date, further *in vitro* imaging of NIH/3T3 cells has been tested under oleylamine-functionalised GO hybrid nanocomposites on zinc-doped AgInS quantum dots (QDs).[68] The confocal imaging illustrated the accumulation of nanocomposites in the cytoplasm or protoplasm within a living cell, which were seen to be circulated around the nucleus. Nanocomposites QDs have displayed brighter fluorescence, lower photobleaching, a thinner photoluminescence spectra, and improved anticorrosion against chemical degradation. Besides, they have demonstrated a higher toxicity level without the therapeutic functions for biomedical applications.[69] To overcome these issues, novel research has created QD-decorated rGO nanocomposites for fluorescent cell imaging and PTT.[70] These nanocomposites have addressed several critical issues, such as QDs toxicity being reduced by surfactant coating and the precise control of the space between the QDs with the rGO. The latter issue is associated with the prevention of fluorescence quenching. Noticeably, QDs-rGO can absorb the NIR irradiation for PTT and cell death, while the absorbed heat simultaneously increases the temperature and decreases the QDs brightness. This becomes a condition allowing the *in situ* measurement of the heat and can indicate the PTT progress. Meanwhile, active targeting and enhanced cell internalisation by conjugated QDs-rGO with targeting or internalisation ligands are demonstrated in Fig. 2. The integration of these astonishing features turns this remarkable nanocomposite into a greater candidate for cancer diagnosis, imaging and treatment *via* drug molecule delivery and PTT.[30]

Nowadays, chemotherapy treatment is the core clinical therapeutic method for curing up to 100 types of cancer, including lung cancer, prostate cancer, lymphoma cancer and breast cancer. However, low therapeutic positive results happen due to drug allergies and limited cellular uptake, as well as other brutal side effects, such as liver and kidney malfunction, a drop in the fertility rate, nerve and muscle effects and cardiac toxicity. These issues will limit the clinical applications of chemotherapy for patients.[71]

PTT mainly works by using laser irradiation, whereby it produces heat elevations and induces the hyperthermia mode towards the tumour tissues. This leads to the denaturation of proteins and disruption of the cell membrane, finally resulting in the irreversible destruction of cancer cells.[72] However, the non-selectivity of tumour tissues and high power density of laser therapy may cause severe side effects to the patient.[73] The

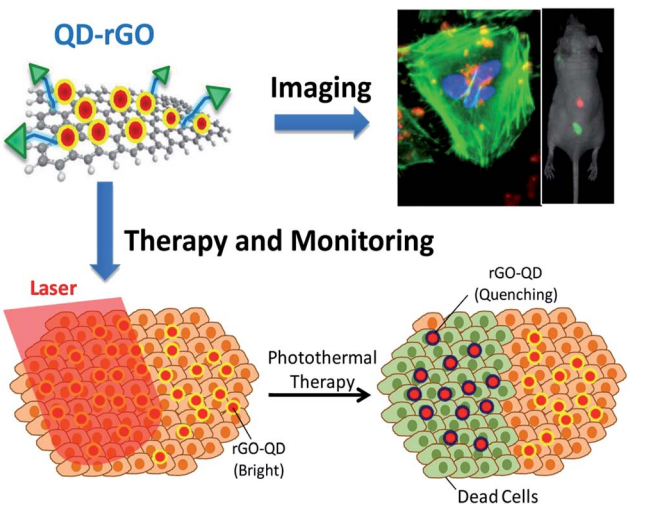


Fig. 2 QDs-rGO nanocomposites implemented against targeted tumour cells can directly indicate bright fluorescence (blue dots) under the assistance of the QDs (top), while NIR radiation was harvested and absorbed on the rGO surface and thus converted into heat, resulting in cancer/healthy cell death together with a reduction of fluorescence (bottom).[30,70]

abilities of PTA to enhance the selectivity of laser absorption is crucial for the heat factor to be easily provided within the microenvironment of a selected tumour tissue that requires a relatively low power density laser signal.[74–82] In this context, GO and rGO materials have been broadly nominated as PTAs for both the *in vitro* and *in vivo* photothermal ablation of cancer cells, which is attributed to their strong light absorbance in the NIR window of the wavelength (*i.e.* in the range of 700–1300 nm).[83–93] Since biological tissues are transparent to such NIR window, a high photothermal conversion efficiency into the tumour tissues will occur due to high-depth light penetration and low tissue-induced light absorption.[94]

Therefore, the incorporation of drug delivery and PTT can enhance the effectiveness of the chemotherapeutic route. So far, the local heterogeneous distribution of heat induced by PTT is not a suitable method to encompass cancer cell death, especially for light-omitted areas.[71] As such, the graphene-based nanomaterial is a brilliant light absorbance agent with a high surface area and can be applied with various therapeutic molecules in order to absorb or conjugate with a tumour. To this end, photothermal chemotherapy is done using DOX-loaded rGO-PEG, which exhibits a higher therapeutic efficacy for *in vivo* cancer treatments in comparison with chemotherapy or PTT alone.[95] Therefore, the epidermal growth factor receptor (EGFR) antibody reinforced PEGylated nano-sized GO (PEG-NGO) was established to deliver epirubicin (EPI) for tumour targeting and triple therapeutics (*i.e.* growth signal blocking, chemotherapy and PTT). This synergistic targeted therapy boosted the local drug concentration by 6.3-fold and yielded ultra-efficient tumour suppression to prolong the survival in mice specimens (>50 days).[30,95]

Recently, a one-pot synthesis route was employed for a relatively new class of photosensitive inorganic nanocomposites that rival liposomes with a combination of hydrophilic and hydrophobic characteristics and have shown superior biocompatibility properties.[96] In general, the useful nanocomposites are made of rGO, mesoporous silicon and amorphous carbon, which are credited with the photon–thermal conversion improvement, active transport drug absorption and cells biocompatibility/penetrability, respectively. The uptake of rGO-based material nanocomposites with a high photothermal conversion efficiency of MDA-MB-231 cells provided a large loading for the hydrophobic drug, (*S*)-(+)-camptothecin (CPT) delivery. According to the current body of knowledge, nanocookie–CPT doses accumulatively remain in liver organ for 24 h after an entire treatment. With the well-assembled rGO-MDA-MB-231 cells nanocomposite, the cancer cell were destructed efficiently without any further side effects *in vitro* and *in vivo*, specifically for both localised drug release and PTT. The results in Fig. 3 confirm the synergistic effect of PBS + NIR as the benchmark (control), CPT + NIR and nanocookie–CPT + NIR, which were compared to the fundamental CPT and NIR. Lastly, the combination of CPT + NIR with nanocookies with a variation of heating temperatures was also evaluated towards tumour-bearing mice *via* MDA-MB231 cell lines.[97]

Recently, the innovative method of the one-pot hydrothermal synthesis of copper sulfide (CuS) nanoplates incorporated rGO (rGO–CuS composite) was employed as a PTA for the ablation of cancer cells.[98] Here, the CuS nanoplates were loaded onto the rGO surface during the hydrothermal process. Consequently, the synthesised rGO–CuS composites dramatically increased the typical optical absorbance in the NIR region, thus improving the photothermal conversion efficiency compared to GO composite and raw CuS nanoplates. Here, researchers attempted to destroy the cancer cells at a relatively high concentration (200 g $mL^{-1}$) and under 980 nm laser irradiation. Then, the *in vitro* cytotoxicity of CuS and rGO–CuS materials on the cancer cells by using the MTT assay for assessing cell metabolic activity was investigated accordingly. In this comprehensive work, the researchers applied CuS and rGO–CuS at various concentrations, while HeLa cells were incubated without any significant toxicity at a low concentration for 24 h. The results showed that the cytotoxicity was directly proportional to the HeLa cell ratio; whereby, when the CuS/rGO–CuS concentration increased, the cytotoxicity also increased. Moreover, the cellular viabilities were estimated to be greater than 80% when the concentrations of CuS and rGO–CuS were increased to 200 g $mL^{-1}$. The results thus suggested that the materials did not impose considerable toxicity to the cancer cells. As shown in Fig. 4, the rGO–CuS composite exhibited higher cytotoxicity in HeLa cells compared to the raw CuS sample, indicating that the former is an effective PTA for cancer treatment.

In Fig. 5, the rGO–CuS composite was observed under confocal microscopy with NIR irradiation of 5 min, specifically under 980 nm NIR at 1 W $cm^{-2}$. The red-coloured dots represent the dead cells at a power density of 1 W $cm^{-2}$, which mediated the highest rate of cell death. Here, almost all the cancer cells were destroyed, as indicated by the laser spot (red colour). Unfortunately, limited dead cells were observed by the raw CuS treatment, thereby the results suggest that the rGO–CuS composite was a more efficient PTA for the ablation of cancer cells.[98]

Similarly, decorated nano-rGO with bovine serum albumin (BSA) was recently developed for use as a PTT system. NS was successfully utilised to suppress breast cancer cells both *in vitro* and *in vivo*.[99] Similar to other photoacoustic NSs,[100] the *in vitro* effect of nano-rGO was tested against MCF-7 cells subjected to an NIR laser at a wavelength of 808 nm and caused apoptosis in the cancer cells in a concentration-dependent manner, as schematically illustrated in Fig. 6. Additionally, the mice administered with the nano-rGO showed thermal cell necrosis.

Obviously, nano-rGOs functionalised with BSA have shown excellent PTT impacts, upon which the NS with an improved passive targeting capacity is introduced for the eradication of different types of solid tumours. The results obtained towards GO-based NS were in agreement with other research works that have shown the detrimental impacts of PEG-rGO on cancer cells.[101] Previously, some *in vivo* studies have shown the value of covalent PEG-GO systems and their impact in large part was based on PTT after high-dosage injections (20 mg $kg^{-1}$) and the implementation of an NIR laser (2 W $cm^{-2}$).[101]

Interestingly, non-covalent PEGylated nano-rGO can absorb noticeably higher NIR than those that are not reduced

 

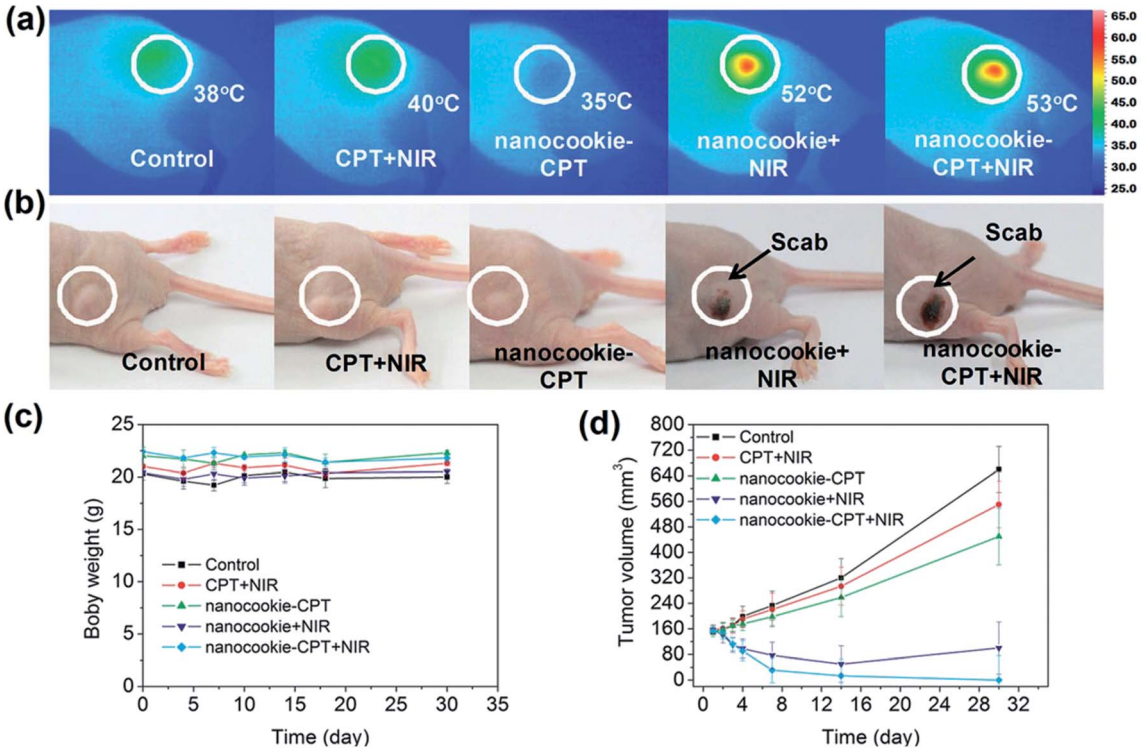


Fig. 3 Infrared thermal images of (a) PBS + NIR (control), CPT + NIR, nanocookie with CPT and NIR, and nanocookie + CPT + NIR with the variation in temperature, (b) the tumour changed into a 'scab' (circled) after treatment with the nanocookie + NIR and nanocookie–CPT + NIR specimens after 4 days, (c) body weight change data with different injections, (d) tumour weight changes after a month.[97]

covalently.[102] Researchers have also revealed that the absorbance volume in the NIR may be a result of recovering p-conjugations in nGO. Besides, the high NIR absorbance of low concentration (20 mg $L^{-1}$) rGO through the use of a low-power laser (*i.e.* 808 nm and 0.6 W $cm^{-2}$) may be regarded as a strong indicator of the nano-rGO's high photothermal capacity. Moreover, the researchers demonstrated that grafting the tripeptide Arg-Gly-Asp (RGD) peptide ligands to nano-rGOs could lead to active targeting results, thus yielding a better/higher photothermal ablation of the infected cells. In addition, nano-rGO has been proven to be able to load non-covalent DOX molecules through p-stacking. Thus, in addition to its capability for surface modifications, nano-rGO has a great potential for combined targeted PTT and chemotherapy.

Recently, Yang and other researchers demonstrated *in vivo* PTT by injecting PEGylated nano-rGO and PEGylated nano-GO

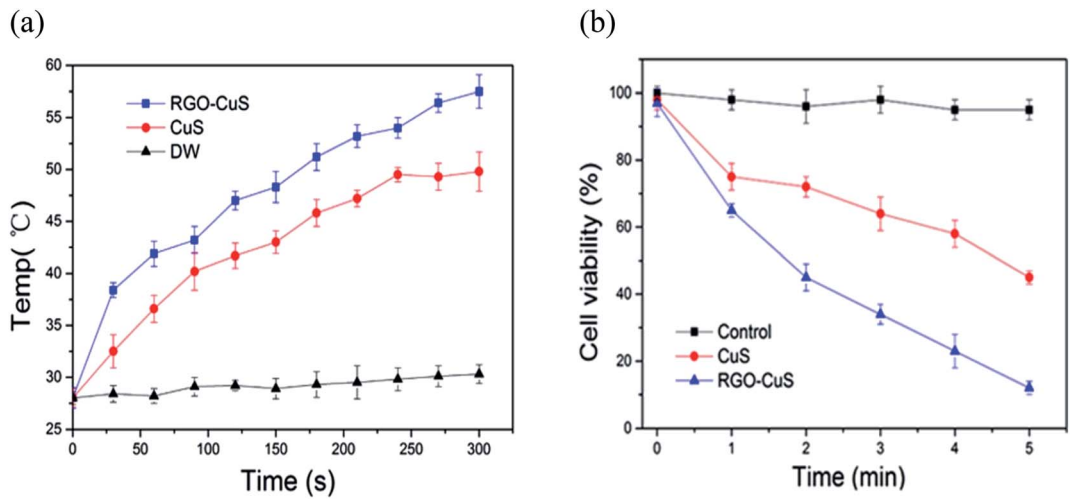


Fig. 4 (a) Temperature changes for CuS incorporated with rGO and (b) cell viability of rGO–CuS as compared with raw CuS.[98]

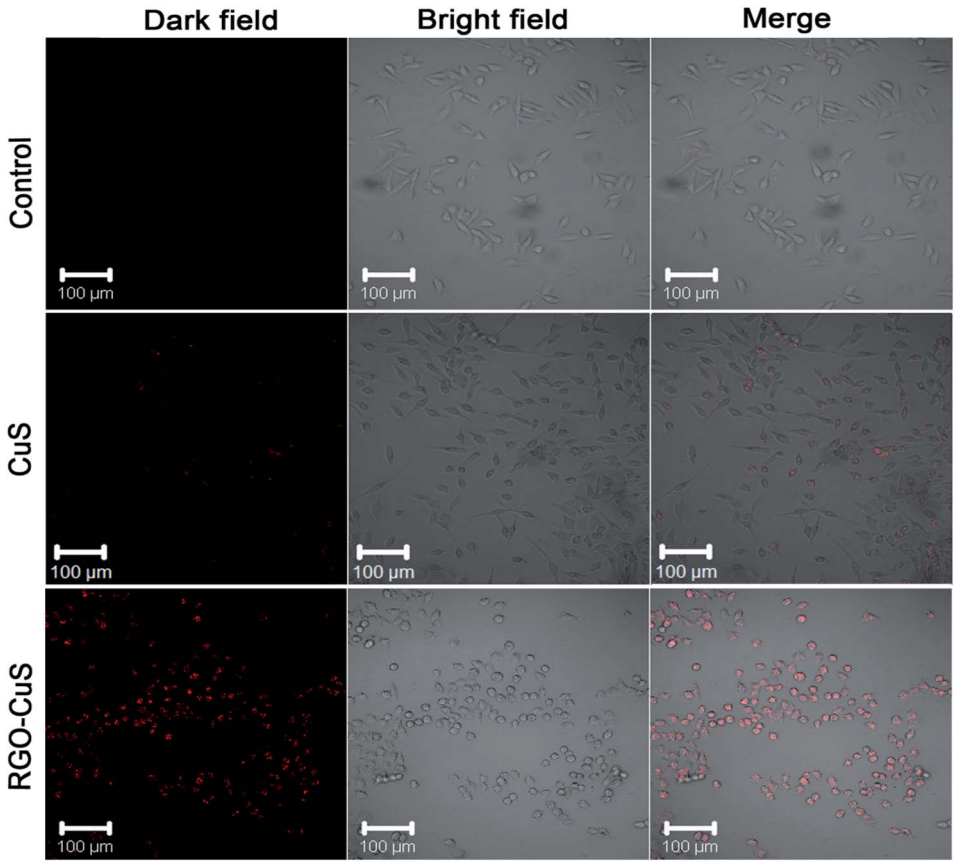


Fig. 5 CLSM images of HeLa cells incubated with DMEM medium, CuS and rGO–CuS composite.[98]

into 4T1 tumour-bearing mice intravenously. Following this, they revealed that the tumour size was significantly reduced, while the survival index was highly improved in the PEGylated nano rGO-treated group that also underwent laser irradiation. In the histological examination of various tissues, no clear toxic effects were found in mice treated with PEGylated nano-rGO.[103]

In another study, non-covalent PEGylation of the nano-rGO sheet was established, derived *via* chemical reduction in order to conjugate a specific quantity of graphene sheets. This offered

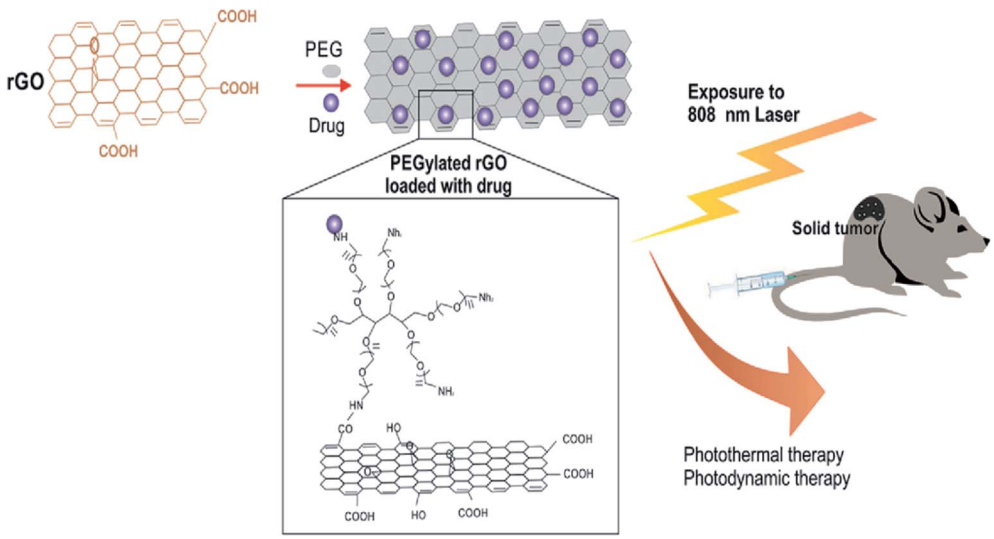


Fig. 6 *In vivo* photodynamic therapy of cancer using PEGylated rGO under 808 nm laser irradiation.[104]

 

an increased NIR absorbance by up to 6-fold. Besides, a few of the rGO sheets with amphiphilic surfactants displayed good stability and biocompatibility in biological buffer solutions. The optimised nano-rGO allowed the peptide conjugation of the targeting cancer cells and selective photoablation at a low dose. These are pioneering outcomes involving the reduced GO form taking part in non-covalent PEGylation for biological applications, thereby resulting in a highly effective PTA with a significant absorbance of NIR light towards carbon-based materials.[32] Research has also developed biocompatible rGO sheets potentially for PTT purposes. Here, the nano-rGO sheets were of a smaller size, spanning ~20 nm, and were developed *via* covalent PEGylation through the sonication route. Furthermore, researchers have determined that the chemical reduction of nano-GO can afford up to 6-fold increase in activity and more; consequently, this improves the NIR absorbance for the PTA, which is also comparable to CNTs and gold-based nanomaterials. Then, they demonstrated the functionalisation of nano-rGO *via* specific targeting ligands for a selective type of cancer cell with photothermal ablation *in vitro*. Attempts were made to try systematic *in vivo* tests with a small dose of nano-rGO for PTT on tumours present in mice bodies and at very low laser power. The result showed that the high NIR absorbance of nano-rGO allowed for the efficient photothermal heating of solutions at low concentrations of nano-rGO (Fig. 7). Additionally, a small concentration of the nano-rGO (~20 mg $L^{-1}$) exhibited rapid photothermal heating, which occurred upon its irradiation by a low-power laser at 0.6 W $cm^{-2}$ (Fig. 8).

## 4. Future perspectives of PTT

A short time after finding the bulk quantity of graphene, its derivatives, such as GO, CNTs and other graphene-based nanomaterials, were considered as low-cost building blocks for advanced methodologies and for the development of medical applications, which are unlimited in imagination. For example, the variety possible with of GO reduction and its incorporation with different materials for building composites and new novel functional materials are indeed endless. Note that polymers and composites have already been added to GO additives, either in their nanoparticle forms for mechanical stabilisation or to facilitate the processing itself. Similarly, graphene is highly compatible biologically and able to function as an active support for mouse fibroblast cells, thus suggesting its use in encapsulating enzymes, serving as a template for DNA-based therapy, or culturing cells.

Furthermore, the uniqueness of both the physical and chemical properties (*i.e.* strong NIR absorption with conjugated π–π surface stacking) of nanographene oxide has led to a dedicated and major amount of works utilising rGO in PTT, yielding a synergistic effect in cancer cell destruction. The assumption is that a similar strategy may also be applied in advanced graphene-based chemotherapies, drug delivery and gene transfection. As graphene, GO and rGO are great drug

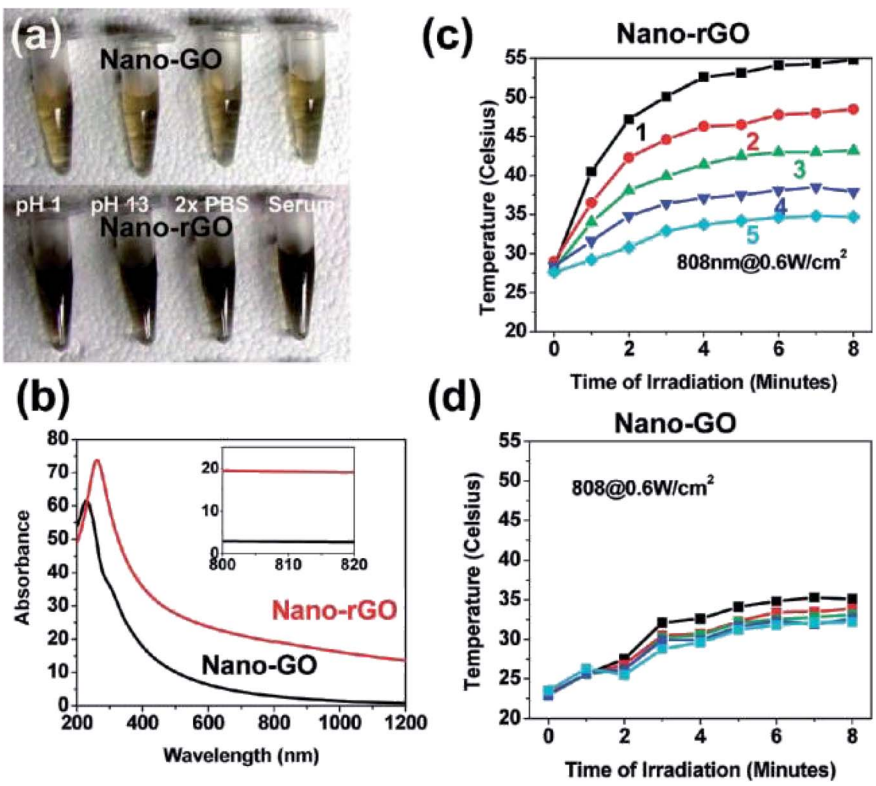


Fig. 7 (a) Samples of the PEGylated-based solutions with covalently formed nano-GO and nano-rGO, (b) UV-vis spectra. Photothermal heating curves of (c) nano-rGO and (d) nano-GO solutions.[32]

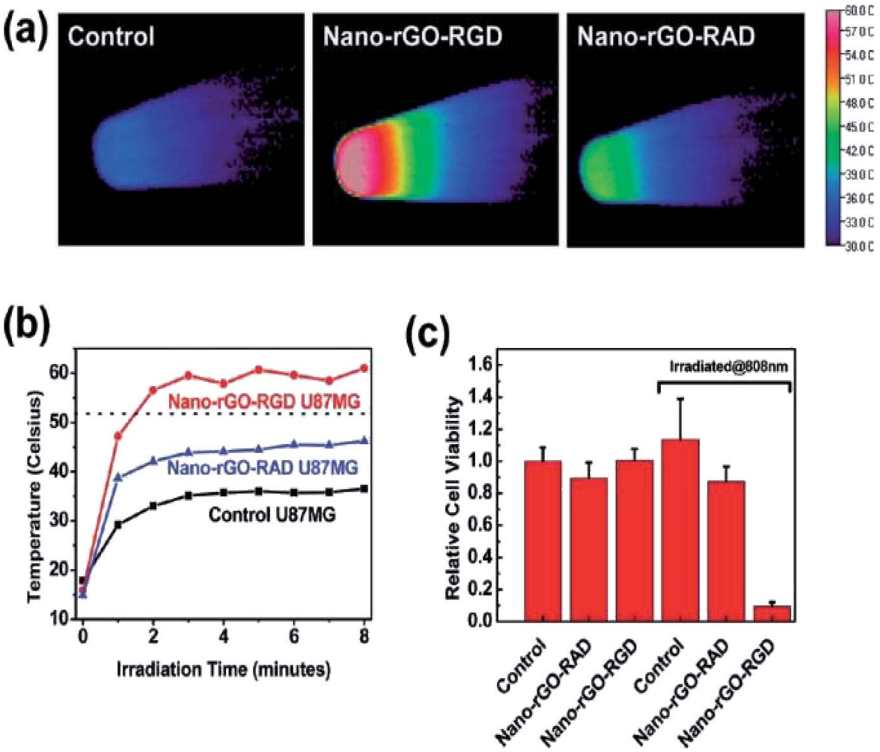


Fig. 8 (a) Thermal images of pellets with nontreated U87MG cells (control specimen shown at left), cells with added nano-rGO-RGD (middle) and cells treated by nano-rGO-RAD (right), respectively, irradiated under an 808 nm laser at a power of 15.3 W $cm^{-2}$ for 8 min duration. (b) Cell pellet heating temperature against irradiation time curves and (c) cell viability after 24 h irradiation.[32]

carriers for anticancer treatments, it is anticipated that in the near future, it will be convenient to combine chemotherapy with PTT for targeted drug delivery and treatment, without the need to use additional drug carriers. Regardless, the low toxicity of nano-GO and rGO has been proven in various research works, rendering the inherent nonbiodegradability of graphene-based materials as the last major concern in clinical applications.

## 5. Conclusion

rGO has attracted great attention for its outstanding properties, and because it can be easily synthesised *via* chemical or mechanical approaches. In contrast, PTT is capable of undertaking thermal ablation against targeted cancer cells. Moreover, numerous established ideas have been suggested regarding graphene-based nanomaterials and their derivatives as aggressively promising and active PTT agents, especially in combination therapies for cancer treatment. Several key ideas were thus reviewed in designing a graphene-based nanostructure with multifunctional PTT or combination therapy abilities in order to achieve efficient treatment for future and advanced clinical purposes. For instance, the combination of physical properties related to a stimuli-responsive targeted drug carrier with a high concentration of PTT is needed in order to develop other treatments. Indeed, graphene could act as a PTA agent and exhibited strong NIR absorbance towards defeating cancer cells. Due to its novelty as a light-absorbing nanoparticle, it could serve for specific therapeutic reagent delivery to a targeted tumour area *via* PTT. Additionally, thermal enhancement of the therapeutic agents incorporated with graphene, instead of applying conventional chemotherapy treatments, could minimise several side effects that a patient may encounter.

## Conflicts of interest

There are no conflicts to declare.

## Acknowledgements

This work was financially supported by Impact-Oriented Interdisciplinary Research Grant (No. IIRG018A-2019), Global Collaborative Programme-SATU Joint Research Scheme (No. ST012-2019), BOLD2025 Grant (No. 10436494/B/2019008), and Internal Research Grant Opex (No. RJO10517919/iRMC/Publication) under Universiti Tenaga Nasional Sdn. Bhd., Malaysia.

## References

1 Y. Liu, *et al.*, Photothermal therapy and photoacoustic imaging via nanotheranostics in fighting cancer, *Chem. Soc. Rev.*, 2019, **48**(7), 2053–2108.
2 S. M. Mousavi, *et al.*, Graphene Nano-ribbon Based high potential and Efficiency for DNA, Cancer therapy and drug delivery applications, *Drug Metab. Rev.*, 2019, 1–35.

 

3 A. Savardashtaki, *et al.*, Core-Shell Nanofibers: A New Horizon in Controlling the Drug Release, *Curr. Cancer Ther. Rev.*, 2017, **13**, 1–26.
4 R. Ravanshad, *et al.*, Application of nanoparticles in cancer detection by Raman scattering based techniques, *Nano Rev. Exp.*, 2018, **9**, 1373551.
5 N. Goodarzian, *et al.*, Modification of Physical, Mechanical and Electrical Properties of Reinforced Epoxy Phenol Novolac with Nano Cobalt Acrylate and Carbon Nanotubes, *Prog. Rubber, Plast. Recycl. Technol.*, 2018, **34**(2), 105–114.
6 S. M. Mousavi, *et al.*, Modification of Polypropylene-Starch Blend by Eggshell Nano-Particle, EVA and Maleic Anhydride to Improve Biodegradability and Thermal Properties, *Int. J. Chem. Sci.*, 2018, **15**, 225.
7 Z. Farazi, *et al.*, Preparation of LDPE/EVA/PE-MA, Nano Clay Blend Composite in the Stage Potassium Sorbate (KS) and Garlic Oil (GO) as an Antimicrobial Substance, *Polym. Sci. U.S.S.R.*, 2018, **4**, 1–12.
8 A. Zakeri, *et al.*, Polyethylenimine-based nanocarriers in co-delivery of drug and gene: a developing horizon, *Nano Rev. Exp.*, 2018, **9**, 1488497.
9 S. M. Mousavi, *et al.*, Development of Clay Nanoparticles Toward Bio and Medical Applications, *Current Topics in the Utilization of Clay in Industrial and Medical Applications*, 2018, pp. 167–191.
10 S. M. Mousavi, *et al.*, Nanosensors for Chemical and Biological and Medical Applications, *Med. Chem.*, 2018, **8**(8), 205–217.
11 J. Pardo, Z. Peng and R. Leblanc, Cancer targeting and drug delivery using carbon-based quantum dots and nanotubes, *Molecules*, 2018, **23**(2), 378.
12 Z. Chen, *et al.*, The advances of carbon nanotubes in cancer diagnostics and therapeutics, *J. Nanomater.*, 2017, **2017**, 1–13.
13 R. D. Bolskar, Fullerenes for Drug Delivery, in *Encyclopedia of Nanotechnology*, ed. B. Bhushan, Springer Netherlands, Dordrecht, 2016, pp. 1267–1281.
14 S. C. Patel, *et al.*, Graphene-based platforms for cancer therapeutics, *Ther. Delivery*, 2016, **7**(2), 101–116.
15 N. Krasteva, *et al.*, Aminated Graphene Oxide as a Potential New Therapy for Colorectal Cancer. Oxidative medicine and cellular longevity, *Oxid. Med. Cell. Longevity*, 2019, **2019**, 1–15.
16 E. Campbell, *et al.*, Graphene Oxide as a Multifunctional Platform for Intracellular Delivery, Imaging, and Cancer Sensing, *Sci. Rep.*, 2019, **9**(1), 416.
17 J. Dong, Anticancer effect and feasibility study of hyperthermia treatment of pancreatic cancer using magnetic nanoparticles, *Oncol. Rep.*, 2011, 719–726.
18 R. Tietze, *et al.*, Nanoparticles for cancer therapy using magnetic forces, *Nanomedicine*, 2012, **7**(3), 447–457.
19 M. Thangamuthu, *et al.*, Graphene-and Graphene Oxide-Based Nanocomposite Platforms for Electrochemical Biosensing Applications, *Int. J. Mol. Sci.*, 2019, **20**(12), 2975.
20 P. Suvarnaphaet and S. Pechprasarn, Graphene-based materials for biosensors: A review, *Sensors*, 2017, **17**(10), 2161.
21 S. F. Kiew, *et al.*, Assessing biocompatibility of graphene oxide-based nanocarriers: a review, *J. Controlled Release*, 2016, **226**, 217–228.
22 H. Su, *et al.*, Aggregation prevention: reduction of graphene oxide in mixed medium of alkylphenol polyoxyethylene (7) ether and 2-methoxyethanol, *RSC Adv.*, 2018, **8**(68), 39140–39148.
23 W. Sun, *et al.*, Preparation, Characterization and Application of Multi-Mode Imaging Functional Graphene Au-Fe3O4 Magnetic Nanocomposites, *Materials*, 2019, **12**(12), 1978.
24 A. N. Nikam, *et al.*, Design and development of thiolated graphene oxide nanosheets for brain tumor targeting, *Int. J. Polym. Mater. Polym. Biomater.*, 2019, 1–11.
25 S. Shi, *et al.*, VEGFR targeting leads to significantly enhanced tumor uptake of nanographene oxide in vivo, *Biomaterials*, 2015, **39**, 39–46.
26 C. England, *et al.*, Radiolabeled long circulating nanoparticles for re-assessing the enhanced permeability and retention effect in peripheral arterial disease, *J. Nucl. Med.*, 2016, **57**(suppl. 2), 65.
27 P. Navya, *et al.*, Current trends and challenges in cancer management and therapy using designer nanomaterials, *Nano Convergence*, 2019, **6**(1), 23.
28 M. K. Rabchinskii, *et al.*, Facile reduction of graphene oxide suspensions and films using glass wafers, *Sci. Rep.*, 2018, **8**(1), 14154.
29 G. Gonçalves, *et al.*, Breakdown into nanoscale of graphene oxide: confined hot spot atomic reduction and fragmentation, *Sci. Rep.*, 2014, **4**, 6735.
30 Y.-W. Chen, *et al.*, Functionalized graphene nanocomposites for enhancing photothermal therapy in tumor treatment, *Adv. Drug Delivery Rev.*, 2016, **105**, 190–204.
31 M. Quinn, T. Wang and S. Notley, Surfactant-exfoliated graphene as a near-infrared photothermal ablation agent, *Biomedical Physics & Engineering Express*, 2018, **4**(2), 025020.
32 J. T. Robinson, *et al.*, Ultrasmall reduced graphene oxide with high near-infrared absorbance for photothermal therapy, *J. Am. Chem. Soc.*, 2011, **133**(17), 6825–6831.
33 J. Han, *et al.*, Photothermal therapy of cancer cells using novel hollow gold nanoflowers, *Int. J. Nanomed.*, 2014, **9**, 517.
34 Y. Cai, *et al.*, Optical nano-agents in the second near-infrared window for biomedical applications, *Chem. Soc. Rev.*, 2019, **48**(1), 22–37.
35 H. Kim and D. Lee, Near-infrared-responsive cancer photothermal and photodynamic therapy using gold nanoparticles, *Polymers*, 2018, **10**(9), 961.
36 C. Christie, *et al.*, Photothermal therapy employing gold nanoparticle-loaded macrophages as delivery vehicles: comparing the efficiency of nanoshells versus nanorods, *J. Environ. Pathol., Toxicol. Oncol.*, 2017, **36**(3), 229–235.

37 A. C. Doughty, *et al.*, Nanomaterial applications in photothermal therapy for cancer, *Materials*, 2019, **12**(5), 779.
38 Z. Sobhani, *et al.*, Photothermal therapy of melanoma tumor using multiwalled carbon nanotubes, *Int. J. Nanomed.*, 2017, **12**, 4509.
39 Y. Zhu, *et al.*, Decorating gold nanostars with multiwalled carbon nanotubes for photothermal therapy, *R. Soc. Open Sci.*, 2018, **5**(8), 180159.
40 L. Shao, *et al.*, Mesoporous silica coated polydopamine functionalized reduced graphene oxide for synergistic targeted chemo-photothermal therapy, *ACS Appl. Mater. Interfaces*, 2017, **9**(2), 1226–1236.
41 X. Chen, *et al.*, Infrared heating of reduced graphene oxide nanosheets as photothermal radiation therapeutic agents for tumor regressions, *Mater. Res. Express*, 2019, **6**(8), 085080.
42 H. Liu, *et al.*, Glucose-reduced graphene oxide with excellent biocompatibility and photothermal efficiency as well as drug loading, *Nanoscale Res. Lett.*, 2016, **11**(1), 211.
43 Y. Pang, *et al.*, Artesunate-modified nano-graphene oxide for chemo-photothermal cancer therapy, *Oncotarget*, 2017, **8**(55), 93800.
44 J. Wu, *et al.*, Photothermal Effects of Reduced Graphene Oxide on Pancreatic Cancer, *Technol. Cancer Res. Treat.*, 2018, **17**, 1533034618768637.
45 R. Lima-Sousa, *et al.*, Hyaluronic acid functionalized green reduced graphene oxide for targeted cancer photothermal therapy, *Carbohydr. Polym.*, 2018, **200**, 93–99.
46 K. Turcheniuk, *et al.*, Plasmonic photothermal cancer therapy with gold nanorods/reduced graphene oxide core/shell nanocomposites, *RSC Adv.*, 2016, **6**(2), 1600–1610.
47 M. S. C. dos Santos, *et al.*, Nanographene oxide-methylene blue as phototherapies platform for breast tumor ablation and metastasis prevention in a syngeneic orthotopic murine model, *J. Nanobiotechnol.*, 2018, **16**(1), 9.
48 J. Yu, *et al.*, Improved anticancer photothermal therapy using the bystander effect enhanced by antiarrhythmic peptide conjugated dopamine-modified reduced graphene oxide nanocomposite, *Adv. Healthcare Mater.*, 2017, **6**(2), 1600804.
49 A. T. Smith, *et al.*, Synthesis, properties, and applications of graphene oxide/reduced graphene oxide and their nanocomposites, *Nano Materials Science*, 2019, **1**(1), 31–47.
50 A. Ahmad, *et al.*, Preparation of a chemically reduced graphene oxide reinforced epoxy resin polymer as a composite for electromagnetic interference shielding and microwave-absorbing applications, *Polymers*, 2018, **10**(11), 1180.
51 M. Zainuddin, *et al.*, Synthesis of reduced Graphene Oxide (rGO) using different treatments of Graphene Oxide (GO), in *IOP Conference Series: Materials Science and Engineering*, IOP Publishing, 2018.
52 F. W. Low, C. W. Lai and S. B. A. Hamid, One-step hydrothermal synthesis of titanium dioxide decorated on reduced graphene oxide for dye-sensitised solar cells application, *Int. J. Nanotechnol.*, 2018, **15**(1–3), 78–92.
53 F. W. Low, *et al.*, An investigation on titanium doping in reduced graphene oxide by RF magnetron sputtering for dye-sensitized solar cells, *Sol. Energy*, 2019, **188**, 10–18.
54 F. W. Low, C. W. Lai and S. B. A. Hamid, Study of reduced graphene oxide film incorporated of $TiO_2$ species for efficient visible light driven dye-sensitized solar cell, *J. Mater. Sci.: Mater. Electron.*, 2017, **28**(4), 3819–3836.
55 F. W. Low, C. W. Lai and S. B. A. Hamid, Surface modification of reduced graphene oxide film by Ti ion implantation technique for high dye-sensitized solar cells performance, *Ceram. Int.*, 2017, **43**(1), 625–633.
56 G. Vinodhkumar, *et al.*, Reduced graphene oxide based on simultaneous detection of neurotransmitters, *Progress in Chemical and Biochemical Research*, 2018, **1**, 40–49.
57 X. Y. Gu, *et al.*, Effect of $TiO_2$-rGO heterojunction on electron collection efficiency and mechanical properties of fiber-shaped dye-sensitized solar cells, *J. Phys. D: Appl. Phys.*, 2018, **52**(9), 1–27.
58 A. Domínguez-Bajo, *et al.*, Myelinated axons and functional blood vessels populate mechanically compliant rGO foams in chronic cervical hemisected rats, *Biomaterials*, 2019, **192**, 461–474.
59 S. Stankovich, *et al.*, Stable aqueous dispersions of graphitic nanoplatelets via the reduction of exfoliated graphite oxide in the presence of poly (sodium 4-styrenesulfonate), *J. Mater. Chem.*, 2006, **16**(2), 155–158.
60 D. Li and R. B. Kaner, Graphene-based materials, *Science*, 2008, **320**(5880), 1170–1171.
61 H. Chen, *et al.*, Mechanically strong, electrically conductive, and biocompatible graphene paper, *Adv. Mater.*, 2008, **20**(18), 3557–3561.
62 S. Stankovich, *et al.*, Synthesis of graphene-based nanosheets via chemical reduction of exfoliated graphite oxide, *Carbon*, 2007, **45**(7), 1558–1565.
63 X. Li, *et al.*, Highly conducting graphene sheets and Langmuir–Blodgett films, *Nat. Nanotechnol.*, 2008, **3**(9), 538.
64 H. A. Becerril, *et al.*, Evaluation of solution-processed reduced graphene oxide films as transparent conductors, *ACS Nano*, 2008, **2**(3), 463–470.
65 X. Li, *et al.*, Simultaneous nitrogen doping and reduction of graphene oxide, *J. Am. Chem. Soc.*, 2009, **131**(43), 15939–15944.
66 G. Williams, B. Seger and P. V. Kamat, $TiO_2$-graphene nanocomposites. UV-assisted photocatalytic reduction of graphene oxide, *ACS Nano*, 2008, **2**(7), 1487–1491.
67 S. J. An, *et al.*, Thin film fabrication and simultaneous anodic reduction of deposited graphene oxide platelets by electrophoretic deposition, *J. Phys. Chem. Lett.*, 2010, **1**(8), 1259–1263.
68 Y. Sheng, *et al.*, Graphene oxide based fluorescent nanocomposites for cellular imaging, *J. Mater. Chem. B*, 2013, **1**(4), 512–521.
69 X. Li, *et al.*, Biocompatibility and toxicity of nanoparticles and nanotubes, *J. Nanomater.*, 2012, **2012**, 1–19.
70 S. H. Hu, *et al.*, Quantum-dot-tagged reduced graphene oxide nanocomposites for bright fluorescence bioimaging

and photothermal therapy monitored in situ, *Adv. Mater.*, 2012, **24**(13), 1748–1754.

71 X. Qin, *et al.*, Folic acid-conjugated graphene oxide for cancer targeted chemo-photothermal therapy, *J. Photochem. Photobiol., B*, 2013, **120**, 156–162.

72 E. S. Shibu, *et al.*, Nanomaterials formulations for photothermal and photodynamic therapy of cancer, *J. Photochem. Photobiol., C*, 2013, **15**, 53–72.

73 X. Huang, *et al.*, Plasmonic photothermal therapy (PPTT) using gold nanoparticles, *Lasers Med. Sci.*, 2008, **23**(3), 217.

74 L. Cheng, *et al.*, PEGylated WS2Nanosheets as a Multifunctional Theranostic Agent for in vivo Dual-Modal CT/Photoacoustic Imaging Guided Photothermal Therapy, *Adv. Mater.*, 2013, **26**(12), 1886–1893.

75 S. S. Chou, *et al.*, Chemically Exfoliated MoS2as Near-Infrared Photothermal Agents, *Angew. Chem., Int. Ed.*, 2013, **52**(15), 4160–4164.

76 P. K. Jain, *et al.*, Review of Some Interesting Surface Plasmon Resonance-enhanced Properties of Noble Metal Nanoparticles and Their Applications to Biosystems, *Plasmonics*, 2007, **2**(3), 107–118.

77 R. Jin, *et al.*, Controlling anisotropic nanoparticle growth through plasmon excitation, *Nature*, 2003, **425**(6957), 487–490.

78 S. Lal, S. E. Clare and N. J. Halas, Nanoshell-Enabled Photothermal Cancer Therapy: Impending Clinical Impact, *Acc. Chem. Res.*, 2008, **41**(12), 1842–1851.

79 M. Li, *et al.*, Using Graphene Oxide High Near-Infrared Absorbance for Photothermal Treatment of Alzheimer's Disease, *Adv. Mater.*, 2012, **24**(13), 1722–1728.

80 S. Thakur and N. Karak, Green reduction of graphene oxide by aqueous phytoextracts, *Carbon*, 2012, **50**(14), 5331–5339.

81 Z. M. Markovic, *et al.*, In vitro comparison of the photothermal anticancer activity of graphene nanoparticles and carbon nanotubes, *Biomaterials*, 2011, **32**(4), 1121–1129.

82 Z. Zhang, *et al.*, Mesoporous Silica-Coated Gold Nanorods as a Light-Mediated Multifunctional Theranostic Platform for Cancer Treatment, *Adv. Mater.*, 2012, **24**(11), 1418–1423.

83 G. Gollavelli and Y.-C. Ling, Multi-functional graphene as an in vitro and in vivo imaging probe, *Biomaterials*, 2012, **33**(8), 2532–2545.

84 S. H. Ku, M. Lee and C. B. Park, Carbon-Based Nanomaterials for Tissue Engineering, *Adv. Healthcare Mater.*, 2012, **2**(2), 244–260.

85 G. Lalwani, *et al.*, Two-Dimensional Nanostructure-Reinforced Biodegradable Polymeric Nanocomposites for Bone Tissue Engineering, *Biomacromolecules*, 2013, **14**(3), 900–909.

86 M. Pumera, Graphene in biosensing, *Mater. Today*, 2011, **14**(7–8), 308–315.

87 S. Sayyar, *et al.*, Covalently linked biocompatible graphene/polycaprolactone composites for tissue engineering, *Carbon*, 2013, **52**, 296–304.

88 B. Tian, *et al.*, Photothermally enhanced photodynamic therapy delivered by nano-graphene oxide, *ACS Nano*, 2011, **5**(9), 7000–7009.

89 C. Wang, *et al.*, Gold Nanoclusters and Graphene Nanocomposites for Drug Delivery and Imaging of Cancer Cells, *Angew. Chem., Int. Ed.*, 2011, **50**(49), 11644–11648.

90 Y. Wang, *et al.*, Nitrogen-Doped Graphene and Its Application in Electrochemical Biosensing, *ACS Nano*, 2010, **4**(4), 1790–1798.

91 K. Yang, *et al.*, Nano-graphene in biomedicine: theranostic applications, *Chem. Soc. Rev.*, 2013, **42**(2), 530–547.

92 K. Yang, *et al.*, In vivo biodistribution and toxicology of functionalized nano-graphene oxide in mice after oral and intraperitoneal administration, *Biomaterials*, 2013, **34**(11), 2787–2795.

93 K. Yang, *et al.*, Multimodal imaging guided photothermal therapy using functionalized graphene nanosheets anchored with magnetic nanoparticles, *Adv. Mater.*, 2012, **24**(14), 1868–1872.

94 Y. Chen, *et al.*, Two-dimensional graphene analogues for biomedical applications, *Chem. Soc. Rev.*, 2015, **44**(9), 2681–2701.

95 W. Zhang, *et al.*, Synergistic effect of chemo-photothermal therapy using PEGylated graphene oxide, *Biomaterials*, 2011, **32**(33), 8555–8561.

96 J. Liu, *et al.*, Synthesis of phospholipid monolayer membrane functionalized graphene for drug delivery, *J. Mater. Chem.*, 2012, **22**(38), 20634–20640.

97 Y. W. Chen, *et al.*, NIR-triggered synergic photo-chemothermal therapy delivered by reduced graphene oxide/carbon/mesoporous silica nanocookies, *Adv. Funct. Mater.*, 2014, **24**(4), 451–459.

98 C. Hu, *et al.*, Preparation of reduced graphene oxide and copper sulfide nanoplates composites as efficient photothermal agents for ablation of cancer cells, *Nano*, 2015, **10**(08), 1550123.

99 Z. Sheng, *et al.*, Protein-assisted fabrication of nano-reduced graphene oxide for combined in vivo photoacoustic imaging and photothermal therapy, *Biomaterials*, 2013, **34**(21), 5236–5243.

100 D.-H. Hu, *et al.*, Hybrid gold–gadolinium nanoclusters for tumor-targeted NIRF/CT/MRI triple-modal imaging in vivo, *Nanoscale*, 2013, **5**(4), 1624–1628.

101 K. Yang, *et al.*, Graphene in mice: ultrahigh in vivo tumor uptake and efficient photothermal therapy, *Nano Lett.*, 2010, **10**(9), 3318–3323.

102 T. Li, *et al.*, One-step reduction and PEIylation of PEGylated nanographene oxide for highly efficient chemo-photothermal therapy, *J. Mater. Chem. B*, 2016, **4**(17), 2972–2983.

103 K. Yang, *et al.*, The influence of surface chemistry and size of nanoscale graphene oxide on photothermal therapy of cancer using ultra-low laser power, *Biomaterials*, 2012, **33**(7), 2206–2214.

104 N. Rahmanian, *et al.*, Recent trends in targeted therapy of cancer using graphene oxide-modified multifunctional nanomedicines, *J. Drug Targeting*, 2017, **25**(3), 202–215.